SINGLE AND DOUBLE SHOCK INITIATION OF EDC37

D A Salisbury, P Taylor and R E Winter
AWE, Aldermaston
Reading
Berkshire, RG7 4PR, UK

R L Gustavsen, S A Sheffield and R R Alcon
Los Alamos National Laboratory
Los Alamos, New Mexico 87545

Experiments have been fired in which the reaction of the HMX based explosive EDC37 is subjected to single and double shocks generated both by plate impact and by explosives. In the plate impact experiments the growth of reaction in the shocked explosive was monitored by embedded particle velocity gauges and shock tracker gauges. Plots showing the rates at which the initial shock and the following reactive wave grow are presented for comparison with PBX 9501, a relatively porous HMX based explosive. It is concluded that the relative contributions made by the "homogeneous" and "heterogeneous" components of reaction build-up are similar for the two explosives. The plate driven double shock experiments show that if the first shock is reactive the explosive is only partially desensitised to the second shock. In the explosively driven experiments reaction was monitored by strain compensated embedded pressure gauges and by laser velocity measurements. The results provide data not only on run distances but also on the reaction which takes place in the shocked but undetonated phase. The data presented clearly shows significant energy release from the shocked but undetonated explosive.

INTRODUCTION

Hydrocodes with suitable reaction models incorporated are routinely used to assess the safety of explosive systems subject to insults with the potential to detonate the explosive. In assessing how an explosive system will respond to an inadvertent impact it is often sufficient simply to know whether or not detonation conditions will be reached in the explosive. In cases when the insult can be approximated as a single shock this can usually be judged from knowledge of the run distance versus applied shock pressure data which can be generated by wedge tests. In such cases a reaction model which correctly predicts the run distance of the explosive may be adequate.

However, real safety scenarios are often much more complex than this simple single shock model. For example when shocks are transmitted through layers which cover the explosive or reflect from the material confining the explosive, the charge may be subjected to more than one shock. Further, precise information on the temporal and spatial distribution of reaction following an impact is sometimes needed. For example, in situations in which (a) the explosive detonates by a run-to-detonation process or (b) the explosive is shocked to a condition which nearly, but not actually, leads to detonation we may need to know the pressure distribution and energy generated in the shocked material. To achieve accurate predictions of energy and pressure generation in this sub-detonation regime we need to be able to model not only the run distance but also the build-up process.

The purposes of this paper are (a) to describe a suite of experiments which provide data on the growth of reaction and generation of energy following single and double shocking of the HMX-based plastic bonded explosive EDC37 and (b) to provide guidance for the development of reaction models by highlighting the key phenomena observed.

EXPERIMENTS

Two classes of experiments are described. These are (a) 1D plate impact experiments in which the reaction in the shock wave is recorded using shock tracker gauges and embedded *velocity* gauges and (b) explosively driven experiments in which reaction is monitored using embedded *pressure* gauges and laser based surface velocity measurements.

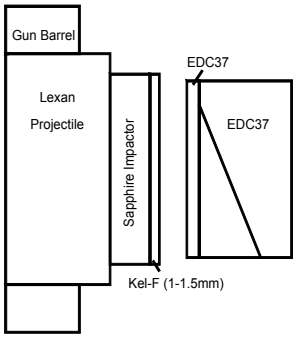

FIGURE 1. SET-UP FOR DOUBLE SHOCK STUDY. EXPERIMENTS ARE FIRED WITH AND WITHOUT EDC37 DISC.

The basic configuration for the plate impact experiments is similar to that described by Vorthman[1] at the 8th Detonation Symposium and subsequently by several other researchers. (See for example references 2-4, 7). The motion of the explosive is measured using electromagnetic particle velocity gauges embedded in the sample at 10 – 12 different depths. In addition to the 10 – 12 particle velocity gauges, these experiments also used "shock tracker" gauges[3]. Outputs from these gauges can be used to construct $x - t$ plots of the shock front position with time. If a transition to detonation occurs within the depth spanned by the shock tracker, the time and distance of the shock-to-detonation transition can be determined.

The configuration for the double shock experiments is similar to that used for the single shock experiments except that, as shown in figure 1, the gun projectile is faced with an impactor disc made of a thin disc of Kel-F, over a thick disc of sapphire. The Kel-F launches a weak wave into the explosive, and the sapphire launches a following stronger wave into the explosive. The strength of the waves is controlled by the impact velocity and the width of the pulse is tailored by using different thicknesses of Kel-F. As with the single shock experiments electromagnetic particle velocity gauges are embedded in the sample at 10 – 12 different depths. Two experiments are done for each stress level/wave width combination. In the first experiment the explosive sample is made without a front disc (a disc is shown in Fig. 1) and the gauges cover depths of 0.0 and 2.5 through 7.0 mm. In the second experiment, a 6 mm thick disc of explosive is used on the front of the sample. The gauges are at depths of 0.0, 6.0, and 6.5 through 11.0 mm. As in the single shock experiments "shock tracker" gauges were used to construct $x - t$ plots of the shock front position.

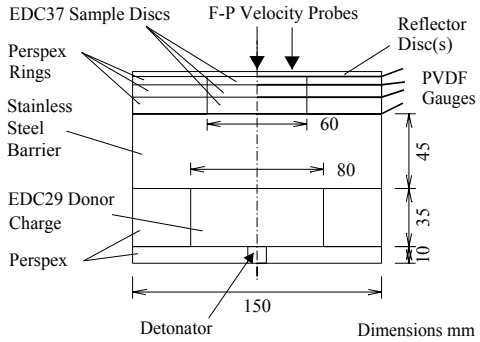

FIGURE 2. SI2D GEOMETRY. EDC37 SAMPLE CONSISTS OF DISCS WITH PRESSURE GAUGES BETWEEN THEM.

The configuration used to study the effect of explosively generated shocks has been described by Winter, Taylor and Salisbury[5]. The shocks delivered to the sample are described below as "single and "double" but, clearly, the waveforms delivered will be complicated by the divergent detonation and the finite lateral dimensions of the geometry. One of the objectives of this configuration was to provide data to test the code's ability to compute more complex situations than those provided by plate impact experiment. To provide data on the response of the EDC37 to single shocks an EDC29 donor charge initiated by a detonator drives a divergent shock wave through a thick stainless steel barrier into an acceptor charge of EDC37 explosive. This sample consists of a set of machined discs with PVDF pressure gauges mounted between them. Other experiments, using the configuration shown in figure 2, studied the response of the explosive to a second shock generated by reflection from a reflector disc. The response of the explosive was measured by embedded pressure gauges and by measuring the

TABLE 1. SINGLE SHOCK PLATE IMPACT EXPERIMENTS

Shot #	*Impact vel. (km/s)*	u_p *(km/s)*	U_s *(km/s)*	*Input Pressure (GPa)*	*Distance to Det. (mm)*
1160	0.608	0.52±0.006	3.65±0.13	3.49±0.16	14.4±0.4
1122	0.682	0.57±0.02	3.70±0.1	3.88±0.17	12.4±0.4
1120	0.809	0.67±0.02	4.00±0.1	4.93±0.19	No result
1159	0.918	0.76±0.02	4.19±0.1	5.86±0.21	7.0±0.4
Ref. 6 #4-233		0.32	3.30	1.96	34.0
Ref. 6 #4-245		0.44	3.50	2.81	24.0
Ref. 6 #4-243		0.56	3.80	3.92	12.0
Ref. 6 #4-199		0.82	4.10	6.16	6.5

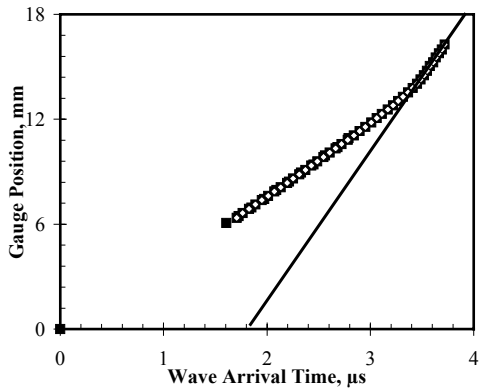

FIGURE 3. SHOT 1160. x-t PLOT SHOWING SHOCK TRACKER AND VELOCITY GAUGE ARRIVAL TIMES.

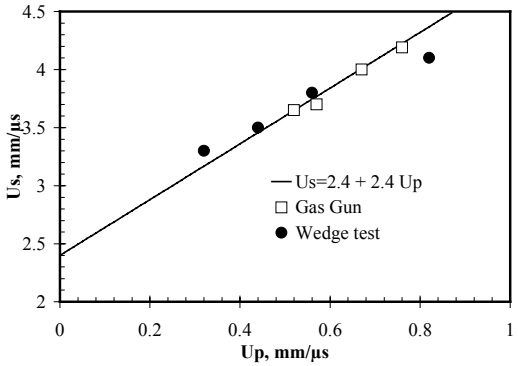

FIGURE 4. HUGONIOT DATA FROM SINGLE SHOCK PLATE IMPACT AND WEDGE TESTS.

surface velocity of the reflector disc. The free surface velocity of the disc was diagnosed with Fabry –Perot velocity interferometry at locations on and off the axis. Control experiments without embedded gauges, with an inert impedance match sample and with a long sample length to determine the run to detonation distance were included in the experimental series.

SINGLE SHOCK PLATE IMPACT

Table 1 summarizes data for all of the single shock plate impact experiments plus data from Wedge Tests fired on EDC37 by Rabie and Harry[6]. The Hugoniot conditions (pressure, shock velocity, particle velocity) and the measured run distance to detonation are presented in the table.

The *x-t* plot showing the position of the shock front with time for shot 1160 is shown in Figure 3. Points from both the shock tracker gauge and the particle velocity gauges are plotted. The slope of the line through the last few data points indicates the detonation velocity. Run distance was obtained from plots such as this using the method described in reference 4. Figure 4 presents Hugoniot data for EDC37[4] along with explosively driven wedge test data. The data is fitted by the Hugoniot Us=2.4+2.4up. Figure 5 shows the run-distance data obtained from our plate impact experiments together with the wedge test data. Also shown for comparison are points obtained in the explosively driven experiments. These will be discussed further later in this paper.

Figure 6 shows wave-profiles from shot 1160 in which EDC37 was impacted with a Vistal impactor at a velocity of 0.608 km/s producing an input of 3.52 GPa. There are twelve wave profiles from gauges located at depths of 0.0, and 6.07 through 10.92 mm. The first profile is from a gauge on the front of the sample and the remaining 11 from embedded gauges.

The input wave is flat topped early on. After about 1.0 µs, the particle velocity at this position begins to gradually decrease indicating reaction is occurring and decelerating the impact interface.

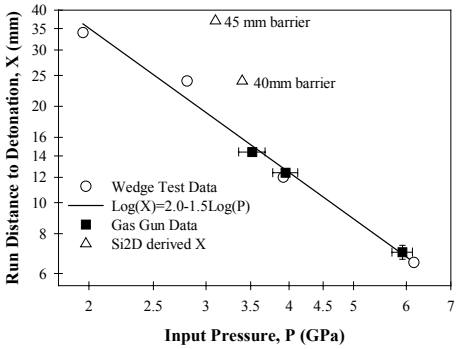

FIGURE 5. RUN DISTANCE DATA FROM SINGLE SHOCK PLATE IMPACT AND EXPLOSIVELY DRIVEN EXPERIMENTS.

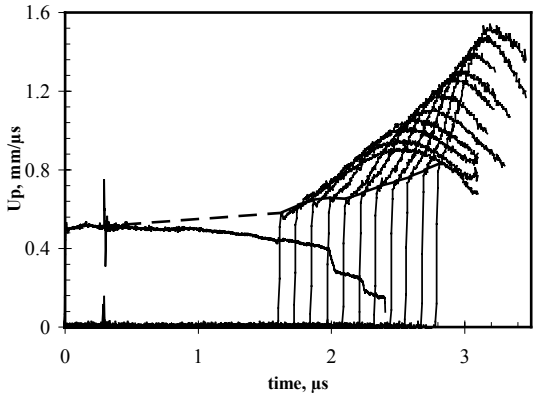

FIGURE 6. Up RECORDS FROM SHOT 1160. THE DASHED LINE PLOTS THE GROWTH OF THE SHOCK. A SIMILAR PLOT (NOT SHOWN) CAN BE CONSTUCTED SHOWING THE GROWTH OF THE PEAK OF THE REACTIVE WAVE.

The other wave profiles show a small increase in amplitude at the shock front and a large following wave, referred to here as the "reactive wave".

Consideration of hot spots suggests that in an explosive with a very low porosity such as EDC37 the "heterogeneous" component of the build up, as exhibited by growth of the shock wave, would play a relatively smaller part in the build up than the "homogeneous" component as manifested by growth of the reactive wave. The dashed line in figure 6 is a plot in the particle velocity-time plane which provides an indicator of the rate of growth of the shock in EDC37 as it propagates into the explosive. A similar indicator of the growth of the reactive wave which follows the shock can be constructed by joining the peaks of the plots of the reactive wave. Figure 7 shows the rates of growth of the shock and the reactive wave for three of the

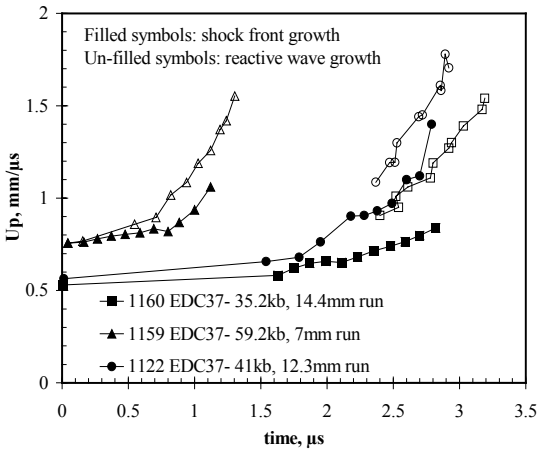

FIGURE 7. SHOWS THE GROWTH OF THE SHOCK AND THE REACTIVE WAVE FOR PLATE IMPACT EXPERIMENTS 1120, 1160 and 1159.

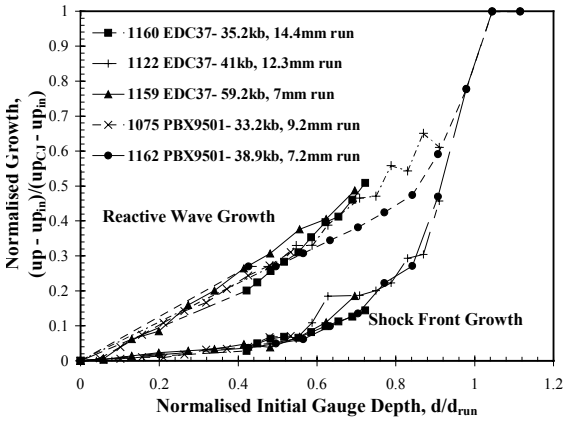

FIGURE 8. COMPARES THE NORMALISED RATE OF GROWTH OF THE SHOCK AND THE REACTIVE WAVE IN EDC37 WITH PBX9501.

single shock experiments. As expected both the shock and the reactive wave grow more rapidly at higher applied shock pressures. An alternative method of presenting the data which provides a comparison of the relative contributions of the shock and reactive wave growth is shown in figure 8. This plot compares the rate of growth of the shock and the reactive wave in EDC37 with the relatively porous and more sensitive HMX based explosive PBX9501[7]. To aid comparison the particle velocities have been normalised. The change in particle velocity from the input particle velocity ($up-up_{IN}$), as a fraction of the total growth ($up_{CJ}-up_{IN}$) is plotted on the vertical axis. The quantity plotted along the horizontal axis is obtained by dividing the original position of the gauge by the run distance. It is seen that the curves

TABLE 2 DOUBLE SHOCK EXPERIMENTS

Shot #	*Impact Velocity (km/s)*	*Kel-F Thickness (mm)*	*1st Shock Pressure (GPa)*	*2nd Shock Pressure (GPa)*	*Run Distance (mm)*	
					From Front Face of target	*From Coalescence*
1175	0.921	1.033	2.87	6.20		
1176	0.925	1.033	2.87	6.20	12.3	6.5
1194	1.170	1.428	3.92	8.56	9.43	2.4
1195	1.165	1.425	3.92	8.56	8.42	2.0

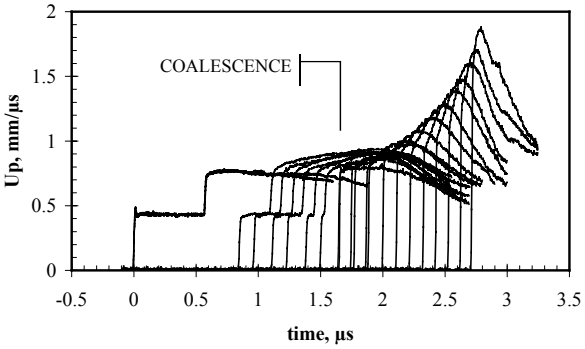

FIGURE 9. RESULTS OF SHOTS 1175 AND 1176 WITH 2.9 AND 6.2 GPa IN THE FIRST AND SECOND SHOCKS.

for the different explosives lie close to one another demonstrating that, even though the sensitivities of the two explosives are different, the *relative* contributions made to the run-to-detonation process by shock and reactive wave growth are very similar. This finding is contrary to our intuition but note that our conclusion here is based on a comparison of only two explosives. We hope to test the hypothesis further by extending the comparison to include a wider range of porosities and compositions.

DOUBLE SHOCK PLATE IMPACT

Wave profiles of particle velocity vs. time and *x-t* plots of the shock trajectories were obtained for two pairs of experiments with wave stresses of 2.9 and 6.2 GPa, and 3.9 and 8.6 GPa. Figure 9 presents velocity gauge data from the pair of lower pressure experiments 1175 and 1176. There are duplicate gauges at the impact surface as well as at 6.0, 6.5, and 7.0 mm. Note that the first wave shows no reaction; the second wave appears to be reacting a little but it is not until the waves coalesce at 5.8 mm and 1.6 μs that the reaction starts to build up significantly.

Figure 10 shows as-measured wave arrival times for experiments 1175 and 1176. From these

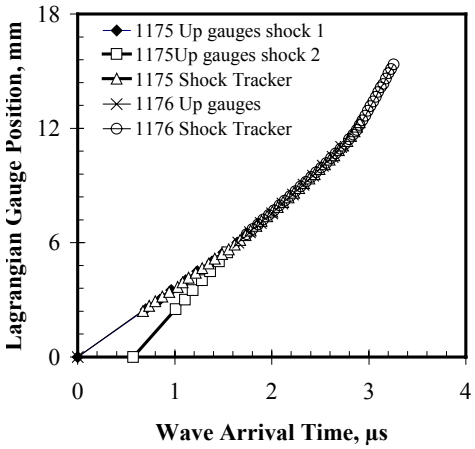

FIGURE 10. x-t PLOT FOR SHOTS 1175 AND 1176 SHOWING THAT THE FIRST SHOCK COALESCES WITH THE FIRST AT 5.8mm.

plots, we can determine *x-t* points for wave coalescence (5.8 mm, 1.6 μs), and the transition to detonation (12.3 mm, 2.9 μs). This is about 1.3 mm beyond the last gauge, which is located at 11.0 mm, and 6.5 mm beyond the position where the first and second shocks coalesce. From Figure 10 we can also determine the velocities of the first and second waves to be 3.6 and 5.6 km/s respectively.

In the next pair of experiments, 1194 and 1195, the effect of significant reaction behind the first shock was investigated. The pulse length between the two shocks was also increased by using a thicker layer of Kel-F, thereby allowing the reaction to run longer. Figure 11 shows the results of these experiments. The stresses of the first and second waves were 3.9 and 8.6 GPa, corresponding to single shock run distances of 13 and 4 mm respectively. Clearly there is significant reaction in both the first and second waves. This is revealed by the positive slopes in particle velocity following the initial shock and by the increase of shock amplitude with depth. The waves coalesce at 7.0 mm. As shown in figure 12 the *x-t* plots from the

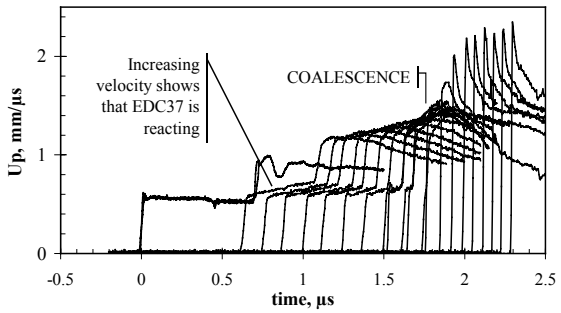

FIGURE 11. RESULTS OF SHOTS 1194 AND 1195 WITH 3.9 AND 8.6 GPa IN THE FIRST AND SECOND SHOCKS.

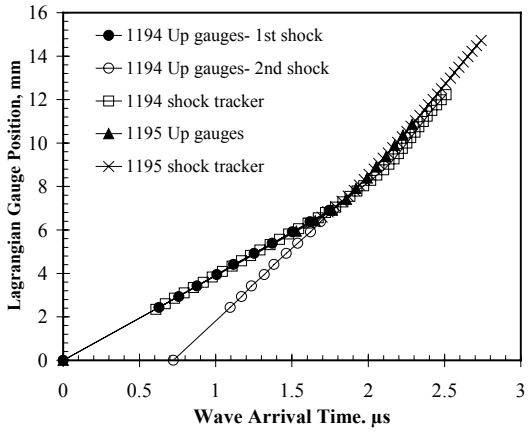

FIGURE 12. x-t PLOT FOR SHOTS 1194 AND 1195 SHOWING THAT THE FIRST SHOCK COALESCES WITH THE FIRST AT 7.0mm.

two experiments did not overlay quite as well as those of Figure 10. Slightly different run distances to detonation of 8.4 mm and 9.4 mm were observed in the two shots. Table 2 summarises the double shock data obtained.

The upright triangles in figure 13 show the run distance data obtained in 1175 and 1176, the unreactive first shock experiments. For the unfilled triangles run distance has been measured from the input face of the explosive sample. For the filled triangles run distance has been measured from the point at which the two waves coalesced. In both cases the pressure is that of the input wave. This pair of shots follows the rule of thumb for double shock experiments: "Build-up to detonation does not begin until after the two waves coalesce."[2]

The higher pressure experiments, 1194 and 1195, are shown as inverted triangles in Figure 13. The unfilled triangles show run distance relative to the front face of the sample and the filled triangles show run distance relative to coalescence. (Note

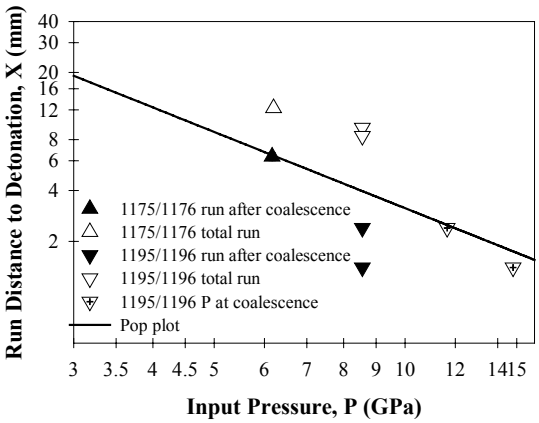

FIGURE 13 RUN DISTANCE DATA FOR DOUBLE SHOCK EXPERIMENTS. THE LINE SHOWS THE POP PLOT OBTAINED FROM THE SINGLE SHOCK EXPERIMENTS.

that there are two points of each type because 1194 and 1195 gave slightly different results). As before the pressure is taken as the pressure of the input wave. The run distance after coalescence is significantly shorter than that predicted by the Pop – plot showing that the explosive is only partially desensitised by the first shock. The points on the right hand side of the chart are plotted using the pressure at coalescence. It is seen that these points lie close to the Pop plot.

The results suggest a modification to the rule that build-up only begins at coalescencse. The total run distance in the case of double shocks is equal to the distance for the two waves to coalesce plus the run distance for the *coalesced* shock. The run distance taken from coalescence can be taken from the single shock pop plot if the *pressure at the moment of coalescence* is used. For weak shocks with insignificant reaction the coalesced pressure can be approximated to the input pressure of the second shock. Strong first or second shocks however will react before coalescence and the resultant shock pressure will be greater than the input pressure. The magnitude of this reactive growth will depend on (a) the initial separation and magnitude of the waves, (b) the velocities of the shock components and (c) the nature of the reactive growth both at the shock front (heterogeneous growth) and the build up behind (homogeneous growth) each shock component. Therefore to accurately model the response of HE to multiple shocks and in particular the total run distance, one must be able to predict the magnitude and form of both homogeneous and heterogeneous components of reaction.

TABLE3. EXPLOSIVELY DRIVEN EXPERIMENTS

Expt.	*Barrier (mm)*	*Sample Material*	*Reflector Material(s)*	*Arrival times at PVDF gauges (μs from shock into acceptor)*					
				10mm	*17.5mm*	*22.5mm*	*32.5mm*	*42.5mm*	*62.5mm*
SI2D/2	60	42.5mm EDC37	40mmSt. Steel	2.83	5.07	6.63	-	13.03	19.86
SI2D/6	40	42.5mm EDC37	40mmSt. Steel	2.68	4.72	5.99	7.42	8.57	-
SI2D/8	40	22.5mm Kel-F	40mm St.Steel	3.62	6.48	8.47	-	-	-
SI2D/10	45	62.5mm EDC37	40mm St.Steel	2.73	4.84	6.24	-	10.86	13.17
SI2D/11	45	22.5mm EDC37	40mm St.Steel	2.77	4.88	6.30	-	-	-
SI2D/12	45	22.5mm EDC37	3mm Al.Alloy 3mm St.Steel	2.70	4.82	6.24	-	-	-
SI2D/13	45	22.5mm Kel-F	3mm Al.Alloy 3mm St.Steel	3.62	6.48	8.67	-	-	-
SI2D/15	45	22.5mm EDC37	3mm Copper	Strain gauges only					
SI2D/16	40	22.5mm Kel-F	40mm St.Steel	Strain gauges only					

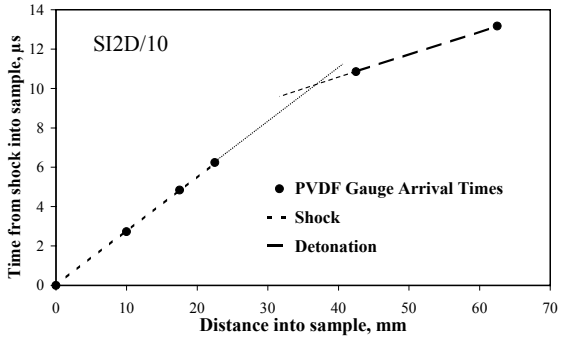

FIGURE 14. SI2D/10 X-T PLOT FROM GAUGE TIMES

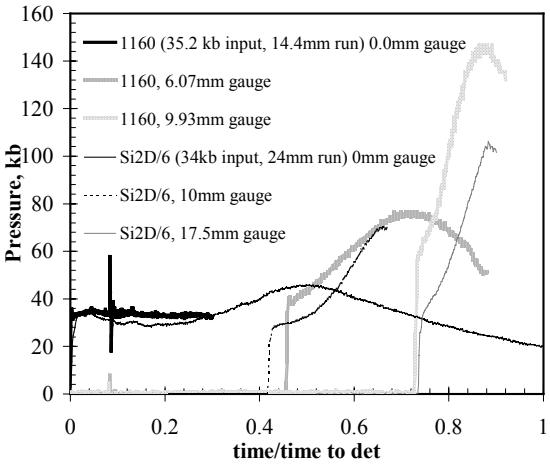

FIGURE 15. COMPARISON OF GAS GUN AND SI2D DATA.

EXPLOSIVELY DRIVEN EXPERIMENTS

The SI2D experiments referred to in this paper are listed in Table 3. Additional experiments fired in this series were listed in references 5 and 8.

The data provided by the explosively driven experiments may be used to support the development of reaction models in a regime which is more representative of real accident scenarios than the regime addressed by the plate impact experiments. A judgement of the effect of departure from truly 1D conditions in the explosively driven experiments may be made by comparing the reaction build-up in the explosively driven and plate impact experiments.

Embedded gauge shock and detonation wave arrival times for the 45 mm barrier experiment, SI2D/10, are shown in Figure 14 from which an effective run distance of 37 mm is derived. A similar analysis yields a run distance of 24 mm for the 40 mm barrier SI2D/6 experiment. Using the measured input pressure for these two experiments allows points to be plotted for comparison with the plate impact experiments as shown in figure 5. It is seen that these run distances are shifted to higher values than for a 1-D experiment. Most of the offset from the 1-D Pop plot run distance observed is probably due to the 2-D divergent shock flow in the experiment, with a small portion of the increased run distance due to the presence of the embedded gauges.

The build-up of reaction in the two types of experiment are compared in figure 15. Figure 15 compares the initiation behaviour of a gas gun experiment (1160) and SI2D/6 which have similar

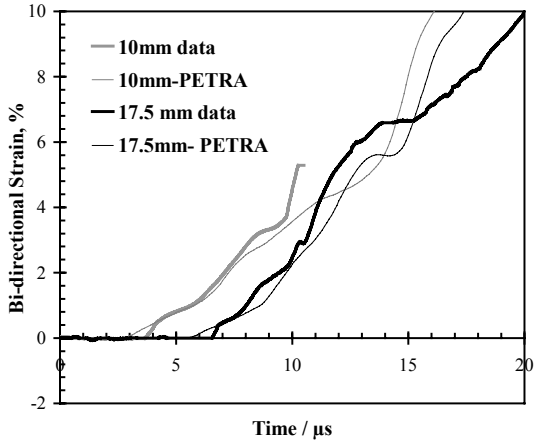

FIGURE 16. SI2D 16 (KEL-F SAMPLE). COMPARES MEASURED AND CALCULATED BI-DIRECTIONAL STRAINS.

peak input pressures and gauges at similar stages of build up to detonation. To aid comparison gas gun particle velocity data has been converted to pressure and the timescale has been normalised to detonation time. The pressure profiles are significantly different with the 2-D geometry showing far less growth at the shock front at a given *percentage* of the run time. However, the pressure gradients in the reactive wave behind the shock front seem to be similar. Since time is normalised to run time in this plot this observation suggests that the reactive wave may control final run distance.

The shocks recorded by the PVDF gauges in the experiments described here are divergent. Therefore the gauges will be subjected to lateral as well as normal strain. We have estimated the strain compensation correction required by using a technique based on the work of Charest and Lilly[9]. An experimental measurement of the strain field experienced by a stress gauge can be made either in the same experiment with a dual gauge package or in a separate nominally identical trial. The latter has been carried out for the 45 mm EDC37 experiments SI2D/12 and 15 and the 40 mm barrier KEL-F experiments SI2D/8 and 16. The strain may also be estimated using a hydrocode. It is seen in figure 16 that hydrocode calculations, using the AWE Eulerian code Petra, of the bi-directional strain at the embedded gauge locations in the KEL-F experiment replicate the measured strain well up to around 5%. An example of the strain compensated pressure data is shown in Figure 17. The profile measured 10 mm into the EDC37 in S2D/12 is shown uncorrected and strain

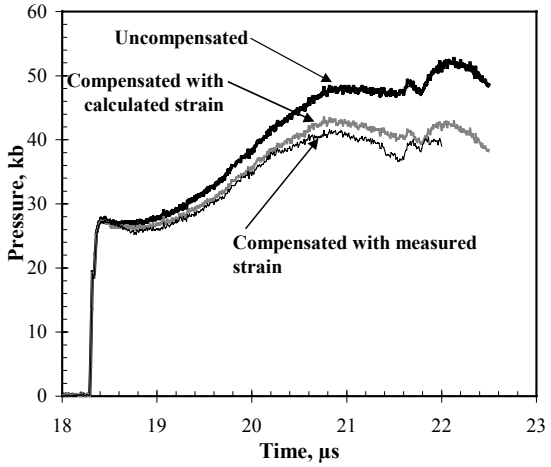

FIGURE 17. SI2D/12. COMPARES UNCOMPENSATED DATA AND STRAIN COMPENSATED DATA USING MEASURED AND CALCULATED STRAINS.

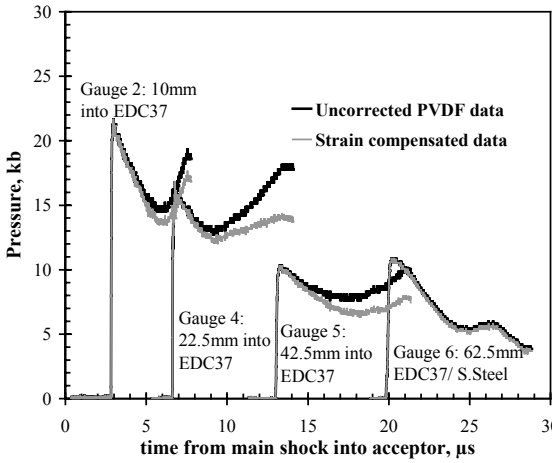

FIGURE 18. STRAIN COMPENSATION APPLIED TO SI2D/2 RESULTS.

compensated using both calculated strain and measured strain as acquired in SI2D/15. It can be seen that although there is a small difference in the profiles derived from the measured and calculated strains they both show a reduction of 10 to 15% from the uncorrected data of the peak pressure.

Calculated strain fields from closely matching reactive burn calculations were used to correct our previously published data[5]. The magnitude of the correction is shown in figure 18 for the less reactive SI2D/2 experiment. Although the relative correction is larger for these lower pressure profiles the general shape of the corrected profiles is not significantly different from the uncorrected data and therefore the main conclusions of previous studies remain unaffected.

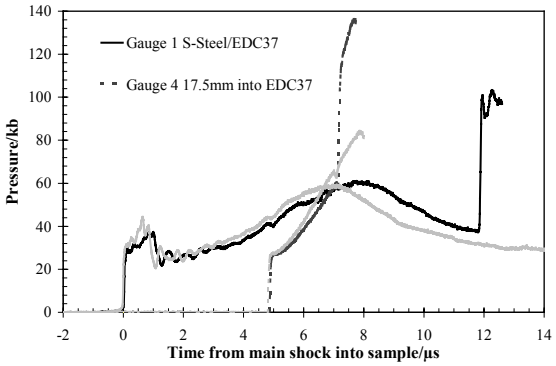

FIGURE 19. COMPARISON OF PVDF GAUGE DATA FROM SI2D/11 –62.5MM SAMPLE (BLACK) AND SI2D/10 –22.5MM SAMPLE (GREY).

Comparison of the pressure gauge data from SI2D/10 and SI2D/11 shows the effect of reflecting the reacting shock wave from a thick high impedance barrier. Figure 19 shows that the reaction profiles before reflection are reasonably reproducible, and the reflection of the shock seems to produce an increase in reaction rate behind the reflected shock. The reflected shock is observed returning to the input face of the sample at a typical shock velocity, well below the normal detonation propagation speed in the explosive. No evidence of detonation on reflection was found.

Figure 20, which compares the experimental free surface velocity measurements from SI2D/12 and SI2D/15, shows the difference in drive from the reacting EDC37 with different strength reflected shocks. A Petra hydrocode calculation in which the EDC37 was modelled with programmed burn and a detonation point to ensure prompt detonation of the acceptor, was performed on the SI2D/12 geometry. The calculated velocity profile, plotted in Figure 20, shows a terminal velocity of 1.75 mm/µs compared to 1.2 mm/µs measured in the SI2D/12 experiment.

The free surface velocity trace on axis for the inert impedance matched Kel-F sample experiment, SI2D/13, is also included in the figure. This shows that the drive given to the Al Alloy S/Steel reflector discs from the donor charge alone with an inert explosive simulant gives a terminal velocity of 0.25 mm/µs. Subtracting the kinetic energy contributed by the donor charge in the Kel-F experiment from the total kinetic energy observed in SI2D/12 and calculated in the detonation calculation, suggests that the extra

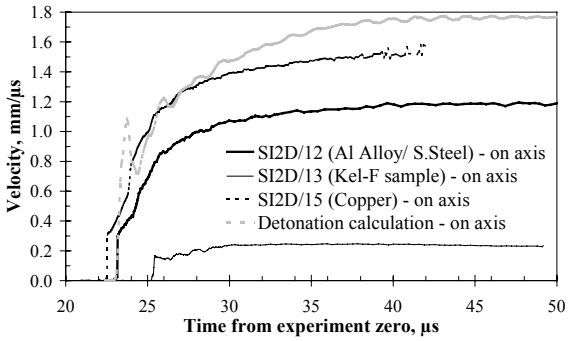

FIGURE 20 . FREE SURFACE VELOCITY MEASUREMENTS AND CALCULATION FOR EXPLOSIVELY DRIVEN DOUBLE SHOCK EXPERIMENTS.

kinetic energy given to the reflector plates by the reacting explosive in SI2D/12 is 46% of that given by the detonation calculation.

The total reflector plate areal masses for the two EDC37 experiments are 3.2g/cm^2 for the Al Alloy S/Steel composite and 2.68g/cm^2 for the Copper reflector. If the total kinetic energy liberated from the reacting explosive plus the donor charge is the same in both experiments, then conservation of kinetic energy predicts a terminal velocity for the Copper experiment, SI2D/15, of close to 1.3 mm/µs. The actual terminal velocity in SI2D/15 is close to 1.5 mm/µs, suggesting that the stronger shock reflected from the higher impedance Copper reflector is liberating a higher percentage of the available energy in the shocked explosive. Subtracting the small contribution from the donor charge from both the SI2D/15 observed kinetic energy and the detonation calculation kinetic energy suggests that the energy release from the shocked but undetonated EDC37 in SI2D/15 is 61% of the calculated detonation drive.

These observations of significant energy release are important when considering the consequences of shock insults to explosives where detonation is not initiated but reaction occurs.

CONCLUSIONS

Plate impact and explosively driven experiments have been conducted to investigate the response of the HMX based explosive EDC37 to shock. The results and analysis summarised in this paper give an insight into the processes and phenomena important in realistic shock insults and highlight specific areas which the modelling will

need to address. It has been shown that the growth of both the shock front and the following reactive wave need to be accurately modelled, especially in situations with multiple shocks. Where full detonation is not established the energy release from the reactive wave can be a significant fraction of the detonation energy.

The relative contributions of heterogeneous and homogeneous growth for different explosives have been compared. Both HMX explosives, EDC37 and the more porous and more sensitive PBX9501, show similar behaviour. This suggests that porosity affects the overall sensitivity but not the character of the build up.

Divergence has been shown to increase run distances as expected. Strain compensated pressure gauge data show that in the SI2D geometry, relative contributions of heterogeneous and homogenous growth are different from the 1-D case. In the divergent geometry growth at the shock front plays a lesser role than observed in 1-D conditions.

Data generated from the 1-D plate impact experiments will aid the development of reactive burn models and the divergent explosively driven studies provide opportunities for benchmarking of hydrocode methodologies in geometries which are more relevant to accident scenarios.

REFERENCES

1. Vorthman, J.E., Andrews, G. and Wackerle, J. "Reaction Rates from Electromagnetic Gauge Data" in Proceedings of the Eighth Symposium (International) on Detonation, Office of Naval Research, Report NSWC MP-86-194, 1986, pp. 99-110.

2. Mulford, R. N., Sheffield S. A. and Alcon R. R., "Initiation of Preshocked High Explosives PBX-9404, PBX9502, PBX-9501, Monitored with In-material Magnetic Gauging", 10th Symp (Int) on Detonation, Boston, Massachusetts, 12-16 July 1993, pp. 459-467.

3. Sheffield, S.A. Gustavsen, R.L., Hill, L.G. and Alcon, R.R. "Electromagnetic Gauge Measurements of Shock Initiating PBX 9501 and PBX 9502 Explosives" in Proceedings of the Eleventh Symposium (International) on Detonation, Snowmass, Colorado, 1998, pp. 451-458.

4. Gustavesen, R. L., Sheffield, S. A., Alcon, R. R., Hill, L. G., Winter, R. E., Salisbury, D. A., and Taylor, P. "Initiation of EDC37 Measured with Embedded Electromagnetic Velocity Gauges", In Shock Compression of Condensed Matter-1999, AIP New York 2000, pp. 879-882.

5. Winter, R. E., Taylor, P. and Salisbury, D. A. "Reaction of HMX-based Explosive caused by Regular Reflection of Shocks", Eleventh Symposium (International) on Detonation, 1998, pp. 649-656

6. Rabie, R. L., and Harry, H. H., "The Characterization of British Explosives FD16, EDC29, EDC35 and EDC37", Los Alamos National Laboratory Report LA-UR-92-1928, 1992.

7. Gustavsen, R.L., Sheffield, S.A., Alcon R.R. and Hill L.G., "Shock Initiation of New and Aged PBX9501 Measured with Embedded Electromagnetic Particle Velocity Gauges", LANL Report: LA-13634-MS, September 1999 (and these proceedings).

8. Taylor, P., Salisbury, D.A., Markland, L., Winter, R.E. and Andrew, M., "Reaction of Shocked but Undetonated HMX-based Explosive", In Shock Compression of Condensed Matter-2001, AIP.

9. Charest, J.A. and Lilly, M.D., "PVF2 Stress Gauges for Non-planar Wave Applications Part 1" Shock Compression of Condensed Matter – 1993, AIP.